

University of Groningen

Light-Responsive Springs from Electropatterned Liquid Crystal Polymer Networks

Ryabchun, Alexander; Lancia, Federico; Katsonis, Nathalie

Published in:
Advanced optical materials

DOI:
[10.1002/adom.202300358](https://doi.org/10.1002/adom.202300358)

IMPORTANT NOTE: You are advised to consult the publisher's version (publisher's PDF) if you wish to cite from it. Please check the document version below.

Document Version
Publisher's PDF, also known as Version of record

Publication date:
2023

[Link to publication in University of Groningen/UMCG research database](#)

Citation for published version (APA):

Ryabchun, A., Lancia, F., & Katsonis, N. (2023). Light-Responsive Springs from Electropatterned Liquid Crystal Polymer Networks. *Advanced optical materials*, 11(12), Article 2300358. Advance online publication. <https://doi.org/10.1002/adom.202300358>

Copyright

Other than for strictly personal use, it is not permitted to download or to forward/distribute the text or part of it without the consent of the author(s) and/or copyright holder(s), unless the work is under an open content license (like Creative Commons).

The publication may also be distributed here under the terms of Article 25fa of the Dutch Copyright Act, indicated by the "Taverne" license. More information can be found on the University of Groningen website: <https://www.rug.nl/library/open-access/self-archiving-pure/taverne-amendment>.

Take-down policy

If you believe that this document breaches copyright please contact us providing details, and we will remove access to the work immediately and investigate your claim.

Downloaded from the University of Groningen/UMCG research database (Pure): <http://www.rug.nl/research/portal>. For technical reasons the number of authors shown on this cover page is limited to 10 maximum.

Light-Responsive Springs from Electropatterned Liquid Crystal Polymer Networks

Alexander Ryabchun,* Federico Lancia, and Nathalie Katsonis*

Future robotic systems will have to adapt their operation to dynamic environments and therefore their development will require the use of active soft components. Bioinspired approaches toward novel actuation materials for active components rely on integrating molecular machines in soft matter, and ensuring that their nanoscale movement is amplified to the macroscale, where mechanically relevant motion is generated. This approach is successfully used in the design of photoresponsive soft springs and other mechanically active materials. Here, this study reports on a new approach where the operation of photoswitches and chiral liquid crystals are combined with an original and mask-free microscopic patterning method to generate helix-based movement at the macroscale, including light-driven winding and unwinding accompanied with inversion of handedness. The microscopic patterning is the result of the unique organization of cholesteric liquid crystals under weak electric field. At a higher level, the pitch and the handedness of the active springs are defined by the imprinted pattern and the angle at which the spring ribbons are cut in the material. These findings are likely to enable soft and responsive robotic systems, and they show how transmission of molecular operation into macroscale functional movement is enabled by materials design across multiple hierarchical levels.

helix-based materials,^[4,5] and as components for soft robotic systems.^[6,7]

Bioinspired approaches toward novel actuating materials for active components rely on integrating molecular machines in soft matter, and ensuring that their nanoscale movement is amplified to the macroscale, where mechanically relevant motion is generated. In earlier work, we have shown that the motion of a molecular photoswitch is amplified in liquid crystal polymer springs and can be used to produce work.^[8,9] These smart springs also adapt their mechanical response to stress, in a manner that mimics muscle fibers.^[10] Other active polymer springs showed promising features in terms of control over motion and also involved liquid crystal polymer materials.^[11–13] The unique property of the liquid crystalline state such as anisotropy of optical, mechanical, and other properties, which can be easily preprogrammed by molecular orientation, holds the key to design active mechanical components for soft robotic systems.^[14–16]


1. Introduction

Helix-based materials are found at all scales of biological systems, arguably because helical organization confers special mechanical properties at multiple length scale, ranging from DNA structures and folded peptides, to plant tendrils, seedpods, muscle fibers, etc.^[1–3] These responsive biological helices have served as an inspiration for the development of active and responsive

Photoswitches are particularly attractive active molecules in this context, because light is a clean and remote source of energy.^[17–21] In particular, integration of photoswitches in chiral nematic layers with a twist organization has led to the design of rich actuation modes.^[8,9,22,23] Bilayered thin films composed of a light-active polymer layer and a mechanically anisotropic passive support layer can also generate active spring shapes.^[24,25] Patterning is another strategy that takes inspiration from the power of movement in plants,^[26] as in seed pods, where moisture-sensitive fibers, accounting for anisotropic mechanical properties, are embedded into an amorphous matrix. We have shown that patterns where isotropic and anisotropic regions alternate can induce powerful movement, for which we used a two-step photopolymerization and mask exposure procedure.^[27] There are a few other works in which the photopatterning of liquid crystal networks has been exploited.^[28–30] These examples are focused to patterns where the liquid crystalline phase and the isotropic phase alternate. However, we propose to use the whole breadth of liquid crystallinity to encode sophisticated patterns for spatial in-plane modulation of molecular alignment,^[31] and argue that these patterns will result in unprecedented actuation of the liquid crystalline soft films.

Here, we demonstrate a new approach to design photoactive polymer springs (**Figure 1a**). The one-step and mask-free strategy

A. Ryabchun, F. Lancia, N. Katsonis
Active Molecular Systems
Stratingh Institute for Chemistry
University of Groningen
Nijenborgh 7, 9747 AG Groningen, The Netherlands
E-mail: a.ryabchun@rug.nl; n.h.katsonis@rug.nl

 The ORCID identification number(s) for the author(s) of this article can be found under <https://doi.org/10.1002/adom.202300358>

© 2023 The Authors. Advanced Optical Materials published by Wiley-VCH GmbH. This is an open access article under the terms of the Creative Commons Attribution-NonCommercial License, which permits use, distribution and reproduction in any medium, provided the original work is properly cited and is not used for commercial purposes.

DOI: 10.1002/adom.202300358

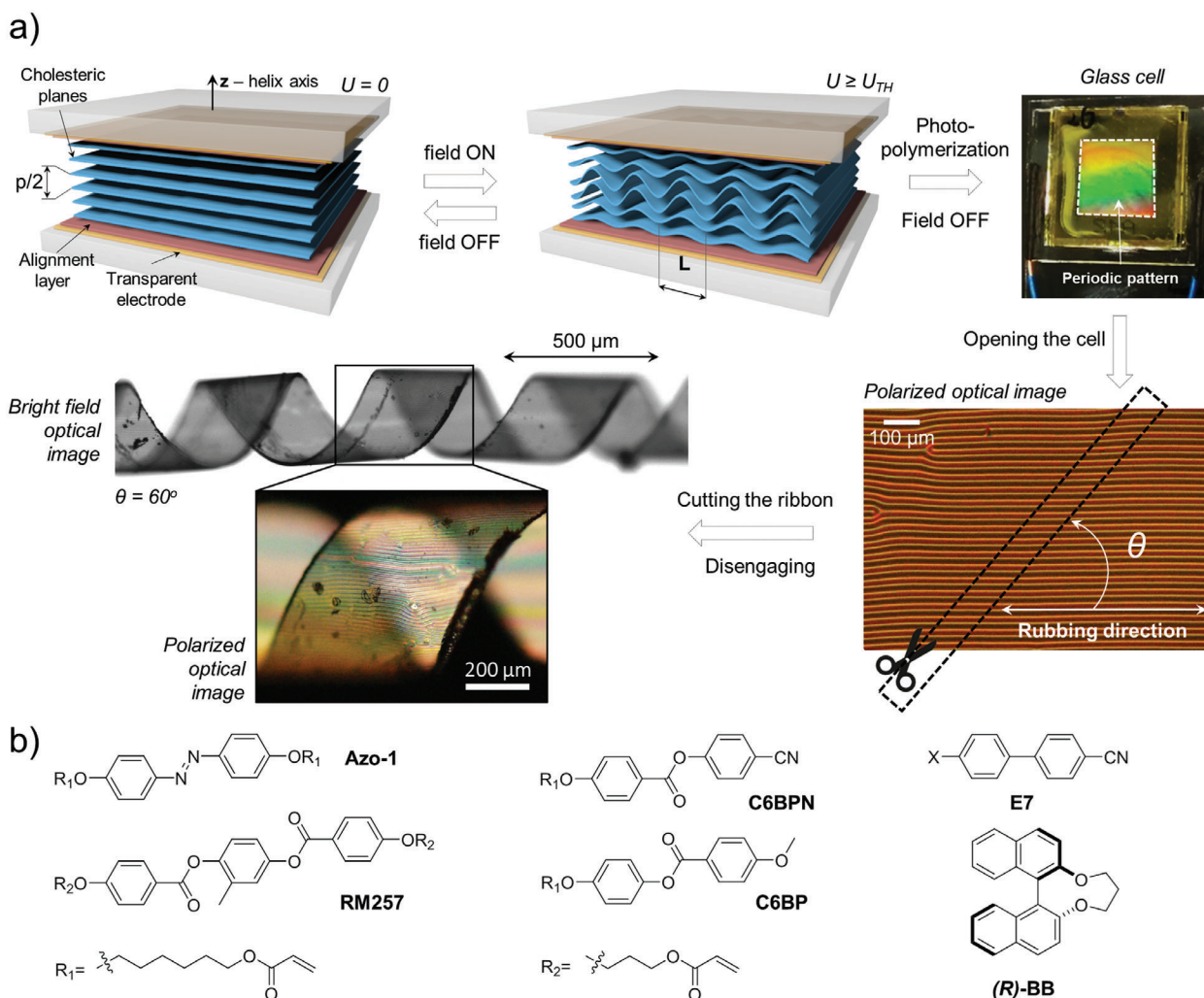


Figure 1. a) General scheme of the fabrication of electropatterned active springs. b) Chemical structure of the components of cholesteric network.

consists in cross-polymerization of well-aligned periodic patterns spontaneously formed in a chiral nematic liquid crystal, upon application of a weak electric field. These patterns are periodic in-plane modulations in the liquid crystal order, and they can be stabilized by post cross-polymerization.^[32] We show that two different electro-induced patterns can be used for the design of active, light-responsive polymer springs that incorporate molecular switches covalently. The pitch and the handedness of the springs are determined by the type of pattern and the angle at which the ribbons are cut. Importantly our work shows that large geometrical changes such as winding, unwinding, and handedness inversion are encoded by molecular-scale chirality.

2. Results and Discussion

2.1. Preparation of Electropatterned Liquid Crystal Polymer Networks

We have designed and synthesized photoactive springs by harnessing the unique response of confined helix-based materials to an electric field.

A thin film of cholesteric liquid crystal with planar alignment is subjected to a weak electric field. Above a threshold voltage (U_{TH}), the cholesteric planes (imaginary planes with unidirectional molecular alignment) undergo in-plane modulation, as shown in Figure 1a schematically. The pattern associated with the resulting modulations is defined by interplay between liquid crystal elasticity, surface anchoring and chiral torque. Therefore, for a given cholesteric material, the pattern can be controlled by the confinement ratio d/P , where d is the thickness of the layer and P is the cholesteric pitch.^[33–36] Among other deformations, we focus on two different linear patterns:^[37] i) the so-called “surface frustrated lying helix” (SFLH) pattern, where the axis of the helices lays in the layer plane, and ii) the Helfrich–Hurault (HH) pattern, in which the helical planes are periodically bent. In both systems, patterns of periodic stripes are formed in the rubbing direction. The high quality and reliable periodicity of these patterns enables optical diffraction gratings.^[34,38–40] The key difference between these two patterns essentially relates to the mechanism of their appearance (nucleation and slow growing for SFLH, and fast development for HH pattern) and in the configuration of liquid crystal director field (see polarized optical images and liquid

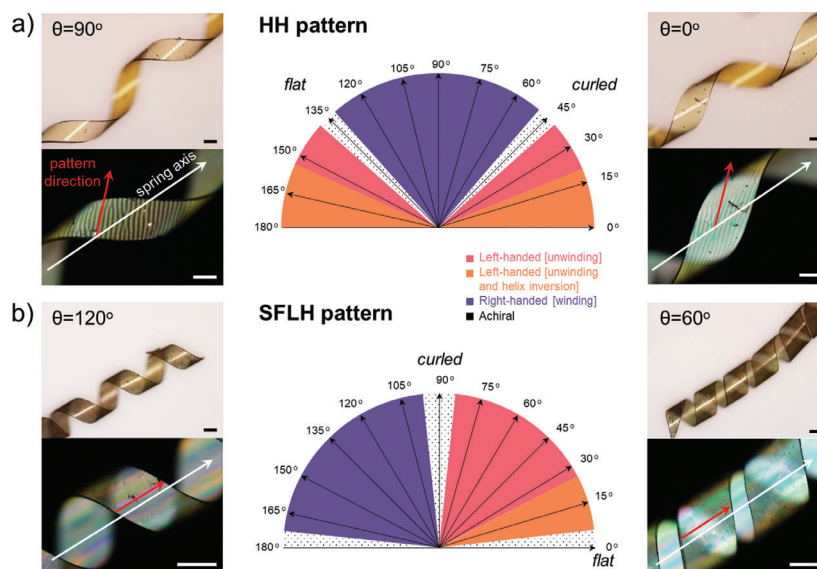


Figure 2. The shape of the ribbons depends on the cutting angle for both the a) Helfrich–Hurault (HH) pattern and b) surface-frustrated lying helix (SFLH). Bright field and polarized optical images of springs. Red arrows indicate direction of the pattern and white arrows indicate the axis of the spring. Scale bars equal to 200 μm .

crystal configuration in Figures S1 and S2, Supporting Information, respectively).

A photopolymerizable chiral nematic liquid crystal was used to design the patterned soft springs (Figure 1b). This liquid crystal is a mixture consisting of liquid crystal acrylates (RM257, 30 wt%, C6BPN, 15 wt%; C6BP, 40 wt%), liquid crystals that reduce the elastic modulus of the postpolymerization material (E7, 10 wt%), and an azobenzene cross-linker (Azo-1, 5 wt%) that is responsible for opto-mechanical feedback. A chiral dopant ((*R*)-BB, 0.05 or 0.25 wt%) was also added, in order to induce with a pitch of 44.7 or 8.9 μm . Once introduced into a 20 μm thick electro-optical cell, the chiral nematic helices experience a confinement ratio of ≈ 0.5 and ≈ 2.2 , which leads to the formation of HH and SFLH patterns, respectively, once low voltage is applied. After photopolymerization with visible light ($\lambda > 420$ nm) under voltage, well-aligned periodic patterns are created in the polymer network, as evidenced by the rainbow colors of the film in the area where the electric field was applied, and where light is diffracted (Figure 1a). The light-induced radical polymerization has the effect of restricting the motion of the molecules composing the liquid crystal, and, in view of the anisotropy of preferred molecular orientation, this movement limitation induces anisotropic in-plane strain. This strain, together with the out-of-plane strain originating from crosslinking density gradient across film thickness, is the driving force for the curling of ribbons after they are cut off from the cell-supported polymerized thin film. Once the cell is opened, the ribbons are cut out at a certain offset angle (θ) in respect to the rubbing direction. Detachment of the ribbon from the glass substrate reveals a polymer spring with clear visible pattern (Figure 1a).

2.2. Generation of Chiral Shapes

We have studied how the spring geometry depends on the cutting angle θ , for each of the two possible patterns (Figure 2). For

the HH pattern, left-handed springs are formed when $-30^\circ < \theta < 30^\circ$, right-handed springs are formed when $60^\circ < \theta < 120^\circ$, and achiral shapes (curled and flat) are revealed at $\theta = \pm 45^\circ$, respectively (Figure 2a). The bright field and polarized optical images of the springs show that the patterns are tilted by $\approx 45^\circ$ with respect to the axis of spring (red and white arrows in Figure 2a). For the other, SFLH pattern, although this pattern is oriented in the same direction as the HH pattern with respect to the rubbing direction, the angular diagram of the spring is entirely different (Figure 2b). The SFLH patterned springs are left-handed $15^\circ < \theta < 75^\circ$ and right-handed at larger angles ($105^\circ < \theta < 165^\circ$). The flat and curled shapes are found at $\theta = 0^\circ$ and $\theta = 90^\circ$, respectively. The SFLH pattern always aligns along the spring axis (Figure 2b).

In addition, we have analyzed the evolution of the pitch of the springs versus cutting angle, θ (Figure 3a,b). The dependence has a tangent-like shape with asymptotes indicated as vertical dashed lines, where pitch of the springs tends to infinite value (i.e., flat shape). So, by passing through these asymptotes the handedness of the spring inverts as well as by passing through zero value of pitch where ribbons are in curled shape. The curves for HH and SFLH patterned springs shifted by 45° in respect to each other which is likely associated with different liquid crystalline organization as it will be addressed further.

2.3. Parameters to Rationalize the Generation of Chiral Shapes

The orientation of the molecules through the thickness of the thin film of liquid crystal polymer network is not trivial, and reaches higher complexity, compared to previous systems generating spiral ribbons.^[8,11,12,27] However, the generation of (chiral) shapes can be understood by considering two key factors simultaneously influencing on internal stresses which result in macroscopic shape morphing: i) Anisotropy of mechanical

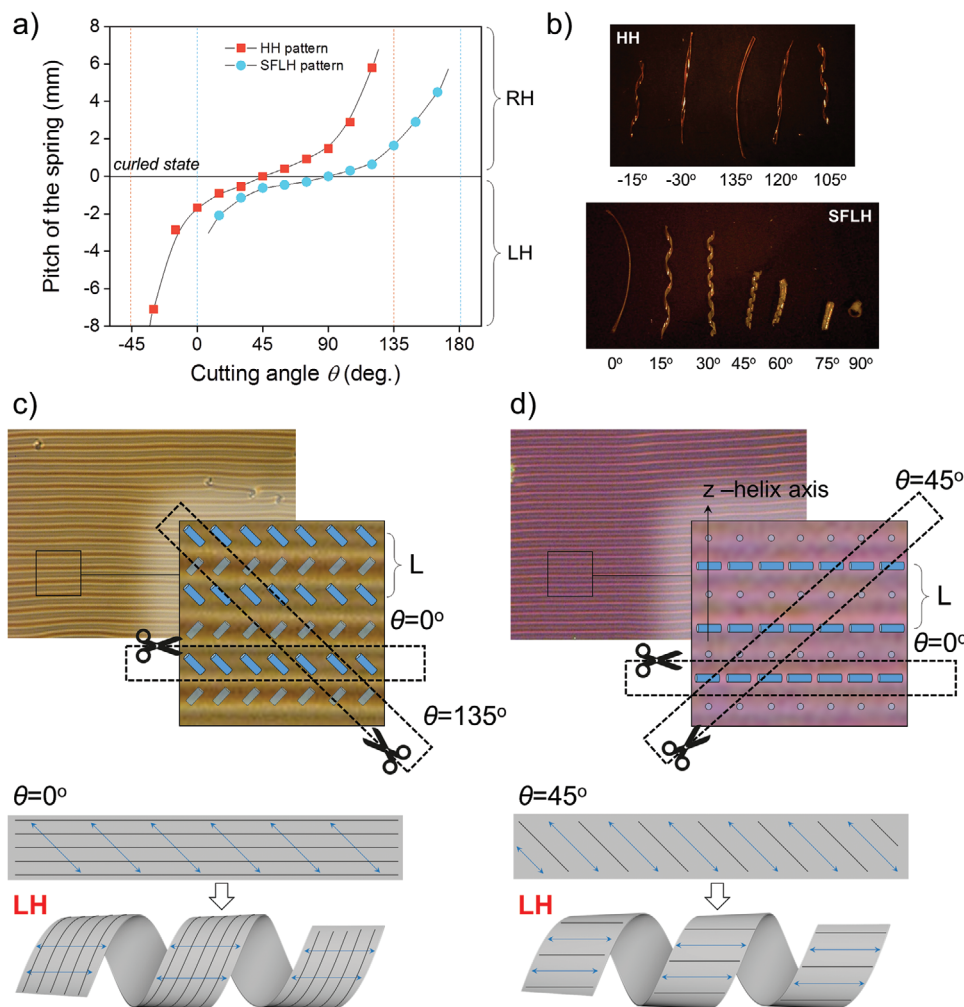


Figure 3. a) The pitch of electropatterned springs is defined by the cutting angle. Positive and negative values correspond to right-handed (RH) and left-handed (LH) helices, respectively. Zero pitch (horizontal line) corresponds to the curled state of the ribbon. Vertical lines show where pitch of the spring is infinite, i.e., the ribbon is flat. b) The photos of springs patterned with HH and SFLH structures. The cutting angles are indicated. c,d) Schematic representation of the liquid crystal organization at midplane in HH and SFLH structures, respectively, overlaid with polarized optical images of those structures. L is one period of the pattern. Molecules lying in the plane of layer are highlighted; molecules having out-of-plane orientation are dimmed. Scheme of the folding of polymer ribbons is shown on the bottom, where back stripes correspond to the lines of pattern and blue arrows—to the average liquid crystal director. The side with drawings corresponds to the stiffer side of the ribbon.

properties which is dictated by liquid crystal configuration. As the distribution of the molecules in the thickness of the thin chiral film is complex, we consider primarily the alignment of the liquid crystal at midplane, i.e., at half-thickness of the thin polymer film, a strategy that has been successfully used for chiral shapes before.^[8,11,12] Figure 3c,d shows the organization of the liquid crystal at midplane, based on previous simulations of similar structures (see Figure S2, Supporting Information).^[37] It is seen that the organization of the molecules is spatially modulated. However, molecules lying in the plane of the layer contribute substantially more to the mechanical properties compared to the molecules oriented perpendicularly to the layer. Importantly, the liquid crystal director in the midplane defines the direction with higher elastic modulus, whereas orthogonal directions are associated with a lower modulus that facilitates bending deformation.^[41] ii) Symmetry breaking element which is repre-

sented by inhomogeneous crosslinking density. A crosslinking density is established across the film thickness due to photopolymerization from one side of the cell and diffusion of monomers during photo-polymerization.^[9,42] The side exposed to visible light during polymerization is more densely crosslinked than the opposite one, and therefore it is stiffer, so this side of the film is always at the outside of the ribbon, to minimize its curvature which is reciprocal to the curvature radius. Once a ribbon is cut out of the cell-supported thin film, the interplay of those two factors brings the ribbon into specific stable macroscopic shape (Figures 2 and 3b).

Our mechanistic interpretation is supported if we consider ribbons with HH and SFLH patterns. In Figure 3c the cut with $\theta = 0^\circ$ has the midplane liquid crystals director which is tilted by 45° in respect to the HH pattern lines (or rubbing direction). The director and therefore direction of larger elastic modulus

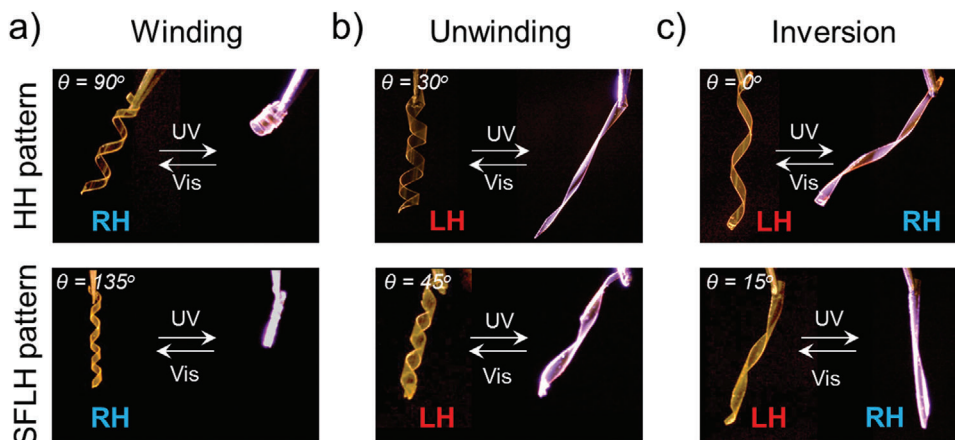


Figure 4. UV light-driven actuation modes of the patterned springs: a) winding, b) unwinding, and c) inversion of handedness. Light source is on the left side of the ribbon.

defines the propagation of the lowest curvature (consequently the highest curvature propagates in orthogonal direction). Here, the stiffer side of the polymer layer is on top of the figure plane and must stay outside the curvature. The ribbon folds into left-handed spring, in order to accommodate these conditions (Figures 2a and 3c). Such interplay of curvatures explains also the flat shape of the ribbon cut out at $\theta = 135^\circ$ where liquid crystal director and therefore the propagation of the lowest curvature coincides with long axis of the ribbon preserving its nearly flat shape.

The liquid crystal configuration in the midplane for cholesteric network with SFLH pattern is presented in Figure 3d. Here we can see that the axis of supramolecular helices (z) lays in the plane of the layer orthogonally to the lines of the pattern as it is indicated in the figure. So, in plane liquid crystal director coincides with the lines which are equivalent to the direction of larger elastic modulus hindering the deformation along this direction as discussed in the previous paragraph. On the other hand, the ribbon can fold in orthogonal direction to the pattern lines which being coupled with gradient of crosslinking density across the thickness makes SFLH patterned ribbons cut out at 45° fold into left-handed spring while ribbon cut out at 0° stays nearly flat (Figure 3d). Interestingly, alignment of the pattern's lines on the spring is always parallel to the spring axis irrespectively handedness and cutting angle (Figure 2b).

2.4. Response of the Polymer Springs to Light

We have investigated the actuation modes of the patterned polymer springs, depending on their geometry. The azobenzene switch that is incorporated in the polymer network covalently is responsible for the actuation. Its *trans*-to-*cis* photo-isomerization on the one hand induces disorder, because the bent-shaped *cis*-isomer is not compatible with the liquid crystalline order, and on the other hand generates mechanical stress by pulling on the network. Moreover, photothermal effect might also contribute to the reduction of liquid crystalline order.^[10,43,44] Thus, the photoisomerization of azobenzene switch causes shape transformation by contraction of the polymer network in the direction of the liquid crystal director, and expansion along the orthogonal direction.

Upon UV illumination, we found that all right-handed springs wind (Figure 4a; Videos S1 and S2, Supporting Information), whereas all left-handed springs unwind (Figure 4b). In all cases the movement is reversible and follows the back isomerization of the molecular switch, thus they can be accelerated with visible light illumination and/or by heating (Figure S3, Supporting Information). At given irradiation condition the motility of the springs is caused by combination of photochemical and photothermal effects^[10] (Figure S4, Supporting Information) and does not depend on the direction of the light source since the light penetration depth is larger than film thickness (only 75% of UV light is absorbed by the film). Both patterns yield similar light-induced behavior which we attribute to the same (*R*)-BB dopant used in both cases, and therefore, a right-handed molecular twist is installed in the thickness of the cell (Figure S2, Supporting Information).

Important to highlight that the electro-induced cholesteric patterns (HH and SFLH) possess not only in-plane modulation of liquid crystal alignment but also right-handed molecular twist that runs across the thickness. We note that the handedness of the twist in the film becomes important in understanding the photoresponse of the springs. As in other studies,^[8,9,27,45] one can understand the response of the system by comparing what is happening in terms of anisotropic shrinking/expansion at the top of the film, with what is happening at the bottom of the film. If the sense of molecular twist corresponds to the sense of the spring handedness we observed macroscopic winding, and on contrary when they are orthogonal then springs demonstrate unwinding, e.g., Winding is the result of accommodation the anisotropic response from expansion of outside face of the ribbon along the axis and contraction of inside face orthogonally.

Remarkably, for relatively small cutting angles θ , left-handed spring invert their chirality under UV exposure as demonstrated in Figure 4c (see also Videos S1 and S2, Supporting Information). Inversion of microscopic handedness of the springs has been observed when the initial pitch of the springs is sufficiently larger than 1 mm (at a given geometrical parameter of the ribbons). The helical movement of the springs in response to light only observed when the springs are made of a chiral material, and we have shown that, in springs made out of (achiral) nematic

polymers, inversion of handedness as well as winding/unwinding cannot be observed (Figure S5, Supporting Information). Overall, and complementarily to approaches based on alternating order-disorder patterns,^[27] the patterning approach that we describe here is a quite simple one-step process which allows simultaneous coexistence of linear in-plane molecular orientation contributing to the macroscopic shape of soft-actuators and molecular twist configuration responsible for the light-induced winding/unwinding. Electropatterned springs have more advanced geometrical features (smaller radius and helical pitch) and larger amplitudes of photoactuations and helix inversion compared to our previously reported springs.^[8,27]

3. Conclusion

We show that the chirality of chiral nematic liquid crystals can be harnessed by a maskless patterning in order to design soft actuators that perform complex helix-based movement at the macroscale. The geometrical patterns of these light-responsive polymer springs (pitch, handedness) can be encoded by design and their actuation modes (winding, unwinding and inversion of handedness) follow the nanoscale movement of the photoswitches that are incorporated covalently. In previous reports, patterns represented alternating areas of isotropic and nematic states of the materials, however here the patterns correspond to an in-plane modulation of the liquid crystal orientation that is formed under low AC voltage. The emergence of chiral shapes has been rationalized by the interplay between i) the mid-plane orientation of liquid crystal molecules accounted for the anisotropy of elastic modulus of the material and ii) the crosslinking gradient throughout the film thickness, which acts as a symmetry breaking element. The springs are designed to reversibly wind, unwind, and even to invert handedness provided that the pitch of spring is long enough (>1 mm), i.e., the initial chiral character is weak. Our findings add to the toolbox of multiscale designs to orchestrate the operation of active molecules across multiple length scales and may serve as active components in soft robotic systems.

4. Experimental Section

The chiral liquid crystal used for the springs is a mixture containing a diacrylate RM257 (30 wt%), monoacrylates C6BP (40 wt%), and C6BPN (15 wt%), crosslinkable azobenzene switch Azo-1 (5 wt%), 10 wt% of low molecular mass liquid crystal E7 (Merck), a small amount (0.25 and 0.05 wt%) of bridged-binol (*R*)-BB^[46] and traces of photoinitiator Irgacure 819 (Ciba). All reactive monomers were purchased from Syntho Chemicals and used as received. The isotropization temperature of this chiral liquid crystal is $T_{iso} = 65$ °C. The cholesteric helix pitch was estimated at 60 °C by using a commercially available wedge cell (E.H.C. Co. Ltd.).^[46]

Design of the Thin Film with HH Pattern: The chiral liquid crystal containing 0.05 wt% of (*R*)-BB was introduced to the planar electro-optical cell of 20 μ m thickness at 70 °C. The substrates of the cell were coated with a polyimide layer, that was later rubbed, in order to promote unidirectional molecular alignment. The sample was slowly cooled down to 60 °C on a heating stage (Instec) and AC voltage (1.5 V, 1 kHz) was applied for 30 min. Then, upon voltage applied, cross-polymerization was initiated with visible light for 2 h (Edmund MI-150 high-intensity illuminator equipped with a cutoff filter, $\lambda \geq 420$ nm). The illumination conditions were purposefully chosen since the visible light is partially absorbed by the azobenzene fragments (Figure S6, Supporting Information) which made the initiation

of polymerization inhomogeneous though the thickness and as a result a crosslinking density gradient across the film thickness was established. After polymerization the voltage was tuned off and the cell was annealed at 60 °C overnight.

Design of the Thin Film with SFLH Pattern: The pattern was obtained in the same way by using monomeric mixture containing 0.25 wt% of (*R*)-BB and at 2.5 V of voltage applied.

The cells were opened and ribbons of 0.3–0.6 mm width were cut out of the polymerized thin film. The cutting angle is defined with respect to the rubbing direction of the cell, when the irradiated side of the film faces the top.

The response of the springs to light was followed using a Dino-Lite USB microscope. An LED lamp $\lambda = 365$ nm (Hönle, intensity ≈ 200 mW cm⁻²) and Edmund MI-150 high-intensity illuminator were used for the actuation experiments. A polarized optical microscope BX51 (Olympus) was used for optical characterization.

Supporting Information

Supporting Information is available from the Wiley Online Library or from the author.

Acknowledgements

The authors acknowledge the European Research Council (Consolidator Grant, Morpheus, 772564) for funding.

Conflict of Interest

The authors declare no conflict of interest.

Data Availability Statement

The data that support the findings of this study are available in the Supporting Information.

Keywords

artificial molecular switches, chirality, liquid crystal networks, liquid crystals, soft robotics

Received: February 13, 2023
Published online: April 7, 2023

- [1] S. J. Gerbode, J. R. Puzey, A. G. McCormick, L. Mahadevan, *Science* **2012**, *337*, 1087.
- [2] S. Armon, E. Efrati, R. Kupferman, E. Sharon, *Science* **2011**, *333*, 1726.
- [3] H. Hofhuis, D. Moulton, T. Lessinnes, A. L. Routier-Kierzkowska, R. J. Bomphrey, G. Mosca, H. Reinhardt, P. Sarchet, X. Gan, M. Tsiantis, Y. Ventikos, *Cell* **2016**, *166*, 222.
- [4] N. Katsonis, E. Lacaze, A. Ferrarini, *J. Mater. Chem.* **2012**, *22*, 7088.
- [5] L. Yin, T. F. Miao, X. X. Cheng, Z. C. Jiang, X. Tong, W. Zhang, Y. Zhao, *ACS Macro Lett.* **2021**, *10*, 690.
- [6] M. P. Da Cunha, M. G. Debije, A. P. Schenning, *Chem. Soc. Rev.* **2020**, *49*, 6568.
- [7] L. Montero de Espinosa, W. Meesorn, D. Moatsou, C. Weder, *Chem. Rev.* **2017**, *117*, 12851.
- [8] S. Iamsaard, S. J. Aßhoff, B. Matt, T. Kudernac, J. J. Cornelissen, S. P. Fletcher, N. Katsonis, *Nat. Chem.* **2014**, *6*, 229.

- [9] S. Iamsaard, E. Villemin, F. Lancia, S. J. Aßhoff, S. P. Fletcher, N. Katsonis, *Nat. Protoc.* **2016**, *11*, 1788.
- [10] F. Lancia, A. Ryabchun, A. D. Nguindjel, S. Kwangmettamat, N. Katsonis, *Nat. Commun.* **2019**, *10*, 4819.
- [11] Y. Sawa, F. Ye, K. Urayama, T. Takigawa, V. Gimenez-Pinto, R. L. Selinger, J. V. Selinger, *Proc. Natl. Acad. Sci. USA* **2011**, *108*, 6364.
- [12] Y. Sawa, K. Urayama, T. Takigawa, V. Gimenez-Pinto, B. L. Mbang, F. Ye, J. V. Selinger, R. L. Selinger, *Phys. Rev. E* **2013**, *88*, 022502.
- [13] A. Ryabchun, F. Lancia, A. D. Nguindjel, N. Katsonis, *Soft Matter* **2017**, *13*, 8070.
- [14] T. J. White, D. J. Broer, *Nat. Mater.* **2015**, *14*, 1087.
- [15] J. Uchida, B. Soberats, M. Gupta, T. Kato, *Adv. Mater.* **2022**, *34*, 2109063.
- [16] K. M. Herbert, H. E. Fowler, J. M. McCracken, K. R. Schlafmann, J. A. Koch, T. J. White, *Nat. Rev. Mater.* **2022**, *7*, 23.
- [17] H. Zeng, P. Wasylczyk, D. S. Wiersma, A. Priimagi, *Adv. Mater.* **2018**, *30*, 1703554.
- [18] A. S. Kuenstler, R. C. Hayward, *Curr. Opin. Colloid Interface Sci.* **2019**, *40*, 70.
- [19] Y. Yu, M. Nakano, T. Ikeda, *Nature* **2003**, *425*, 145.
- [20] H. K. Bisoyi, Q. Li, *Chem. Rev.* **2016**, *116*, 15089.
- [21] A. Ryabchun, N. Katsonis, in *Molecular Photoswitches: Chemistry, Properties, and Applications*, Vol. 2 (Ed: Z. L. Pianowski), Wiley-VCH, Weinheim, Germany, **2022**, Ch. 26.
- [22] J. J. Wie, M. R. Shankar, T. J. White, *Nat. Commun.* **2016**, *7*, 13260.
- [23] A. Ryabchun, F. Lancia, N. Katsonis, *ACS Appl. Mater. Interfaces* **2021**, *13*, 4777.
- [24] X. Lu, S. Guo, X. Tong, H. Xia, Y. Zhao, *Adv. Mater.* **2017**, *29*, 1606467.
- [25] R. C. Verpaalen, M. Pilz da Cunha, T. A. Engels, M. G. Debije, A. P. Schenning, *Angew. Chem., Int. Ed.* **2020**, *59*, 4532.
- [26] C. Darwin, F. Darwin, *The Power of Movement in Plants*, Cambridge University Press, Cambridge, UK, **2009**.
- [27] S. J. Aßhoff, F. Lancia, S. Iamsaard, B. Matt, T. Kudernac, S. P. Fletcher, N. Katsonis, *Angew. Chem., Int. Ed.* **2017**, *56*, 3261.
- [28] L. Liu, B. Geng, S. M. Sayed, B. P. Lin, P. Keller, X. Q. Zhang, Y. Sun, H. Yang, *Chem. Commun.* **2017**, *53*, 1844.
- [29] V. Gimenez-Pinto, F. Ye, *RSC Adv.* **2019**, *9*, 8994.
- [30] F. Ge, Y. Zhao, *Adv. Funct. Mater.* **2020**, *30*, 1901890.
- [31] O. D. Lavrentovich, *Proc. Natl. Acad. Sci. USA* **2018**, *115*, 7171.
- [32] R. A. M. Hikmet, B. H. Zwerver, D. J. Broer, *Polymer* **1992**, *33*, 89.
- [33] V. G. Chigrinov, V. V. Belyaev, S. V. Belyaev, M. F. Grebenkin, *Sov. Phys. JETP* **1979**, *50*, 994.
- [34] A. Ryabchun, A. Bobrovsky, J. Stumpe, V. Shibaev, *Adv. Opt. Mater.* **2015**, *3*, 1462.
- [35] D. Subacius, S. V. Shiyanovskii, P. Bos, O. D. Lavrentovich, *Appl. Phys. Lett.* **1997**, *71*, 3323.
- [36] H. K. Bisoyi, T. J. Bunning, Q. Li, *Adv. Mater.* **2018**, *30*, 1706512.
- [37] A. Ryabchun, A. Yakovlev, A. Bobrovsky, N. Katsonis, *ACS Appl. Mater. Interfaces* **2019**, *11*, 10895.
- [38] H. C. Jau, Y. Li, C. C. Li, C. W. Chen, C. T. Wang, H. K. Bisoyi, T. H. Lin, T. J. Bunning, Q. Li, *Adv. Opt. Mater.* **2015**, *3*, 166.
- [39] D. Subacius, P. J. Bos, O. D. Lavrentovich, *Appl. Phys. Lett.* **1997**, *71*, 1350.
- [40] B. I. Senyuk, I. I. Smalyukh, O. D. Lavrentovich, *Opt. Lett.* **2005**, *30*, 349.
- [41] M. Warner, E. M. Terentjev, *Liquid Crystal Elastomers*, Oxford University Press, Oxford, England **2003**.
- [42] C. L. van Oosten, D. Corbett, D. Davies, M. Warner, C. W. Bastiaansen, D. J. Broer, *Macromolecules* **2008**, *41*, 8592.
- [43] M. Lahikainen, H. Zeng, A. Priimagi, *Nat. Commun.* **2018**, *9*, 4148.
- [44] F. Lancia, A. Ryabchun, N. Katsonis, *Nat. Rev. Chem.* **2019**, *3*, 536.
- [45] Y. Xiao, Z. Jiang, L. Yin, J. Jiang, Y. Zhao, *J. Mater. Chem. C* **2021**, *9*, 16566.
- [46] T. Orlova, F. Lancia, C. Loussert, S. Iamsaard, N. Katsonis, E. Brasselet, *Nat. Nanotechnol.* **2018**, *13*, 304.